molbank

MDPI

Short Note

[μ-1,2-Bis(diphenylphosphino)ethane-κ^2P,P']bis(3-mercapto-1,2-propanediolato-κS-gold(I))

Taichi Baba and Nobuto Yoshinari *

Department of Chemistry, Graduate School of Science, Osaka University, Osaka 560-0043, Japan
* Correspondence: nobuto@chem.sci.osaka-u.ac.jp

Abstract: A new dinuclear gold(I) complex, possessing a bridging diphosphine ligand (1,2-bis (diphenylphosphino)ethane) and two terminal thiol ligands (1-thioglycerol), was synthesized and fully characterized by IR, ^{1}H and ^{31}P NMR, fluorescence, ESI-mass, and diffuse reflection spectroscopy, together with X-ray diffraction and elemental analyses. The compound formed a 1D chain supramolecular structure through intermolecular aurophilic interactions in the crystal structure, leading to photoluminescence in the solid state.

Keywords: gold complex; phosphines; thioglycerol; aurophilic interaction

1. Introduction

1-Thioglycerol (3-mercapto-1,2-diol; H_3tg) is one of the simplest mercapto-diols with one -SH and two -OH groups. H_3tg is highly water soluble and has low volatility compared to other low-molecular-weight thiols, so it has been utilized as a reducing agent for S-S bonds in biomolecules [1] or a potential drug [2]. H_3tg is also available as a protecting reagent for the aqueous synthesis of metal or metal chalcogenide nanoclusters, e.g., CdS [3], CdSe [4,5], CdTe [6], ZnO [7], ZnS [8], HgTe [9], TiO_2 [10], Bi_2O_3 [11], and Au [12–15]. In coordination chemistry, the reactivity of H_3tg toward most transition metal ions was investigated based on spectroscopic characterization [16–18], but the accurate coordination mode of H_3tg was uncertain until the late 20th century because of the lack of single-crystal X-ray diffraction analysis. In 1995, Weller and coworkers reported that the deprotonated H_2tg^- ligand readily binds with Cd^{2+} ions in a μ_2-κS mode to form an infinite 3D coordination polymer in $[Cd(\mu\text{-}H_2tg\text{-}S)_2]_\infty$ [19] (Figure S1a). This was the first crystallographic study on the coordination behavior of H_3tg. After Weller's pioneering research, four metal complexes of H_3tg have been structurally characterized. A similar μ_2-κS bridging coordination mode of H_2tg^- was also detected in a dinuclear gold(I) complex, $[Au_2(PPh_3)_3(\mu\text{-}H_2tg\text{-}S)]$ [20], in which H_2tg^- ligand bridges linear $\{Au(PPh_3)\}^+$ and trigonal $\{Au(PPh_3)_2\}^+$ moieties through the S atom (Figure S1b). Tekeste and Vahrenkamp designed a Zn^{II} complex having a tripodal ligand and H_2tg^-, $[Zn(H_2tg\text{-}S,O)(Tp^{PhMe})]$ (Tp^{PhMe} = tris(3-phenyl-5-methylpyrazolyl)borate) [21], as a model compound of zinc enzyme inhibition by H_3tg. In the Zn^{II} complex, H_2tg^- bound to the Zn^{II} center in a bidentate-*S*,*O* mode (Figure S1c). Tasiopoulos and coworkers reported that the single-crystal-to-single-crystal incorporation of H_3tg into lanthanide MOFs gave H_3tg-decorated MOFs, $[Ln_2(CIP)_2(H_3tg\text{-}O)_2(H_2O)_2]$ (Ln = Nd, Eu; H_3CIP = 5-(4-carboxybenzylideneamino)isophthalic acid) [22,23], in which H_3tg adopted the monodentate-κO coordination mode for Ln^{3+} and one -OH, and one -SH groups remained uncoordinated (Figure S1d). These structural studies indicated that both -SH and -OH groups of H_3tg are potential metal binding sites. However, the non-bridging monodentate-κS, one of the most ubiquitous thiolate coordination modes [24], has yet to be observed for H_3tg.

As an extension of our previous study on the development of diphosphine-bridged digold(I) complexes with two terminal thiolates as the metalloligand [25], we synthesized

check for updates

Citation: Baba, T.; Yoshinari, N. [μ-1,2-Bis(diphenylphosphino)ethane-κ^2P,P']bis(3-mercapto-1,2-propanediolato-κS-gold(I)). *Molbank* **2023**, *2023*, M1698. https://doi.org/10.3390/M1698

Received: 27 June 2023
Revised: 15 July 2023
Accepted: 18 July 2023
Published: 19 July 2023

Copyright: © 2023 by the authors. Licensee MDPI, Basel, Switzerland. This article is an open access article distributed under the terms and conditions of the Creative Commons Attribution (CC BY) license (https://creativecommons.org/licenses/by/4.0/).

the title compound, $[Au_2(dppe)(H_2tg\text{-}S)_2]$ (**1**; dppe = 1,2-bis(diphenylphosphino)ethane), in this work. Single-crystal X-ray analysis of **1** revealed that two deprotonated H_2tg^- ligands are spanned by a linear $\{Au_2(dppe)\}^{2+}$ moiety, and each H_2tg^- ligand binds to the Au^I center in a non-bridging monodentate-κ*S* mode. The dinuclear complex **1** was connected by intermolecular aurophilic interactions [26,27], forming a 1D chain structure in the crystal lattice. Complex **1** was fully characterized by powder X-ray diffraction (PXRD) analysis, elemental analysis, and various spectroscopic measurements, including X-ray fluorescence, IR, ^{1}H NMR, ^{31}P NMR, diffuse reflection, ESI-mass, and emission spectra.

2. Results and Discussion

2.1. Synthesis and Characterization of **1**

The 1:2:2 reaction of $[Au_2Cl_2(dppe)]$ [28], H_3tg, and KOH in EtOH/H_2O gave a pale-yellow powder of **1** in a moderate yield (47 %) (Figure 1). The elemental analysis data of **1** agreed with the formula of a 1:2 adduct of $\{Au_2(dppe)\}^{2+}$ and H_2tg^- without any counter ions or solvent molecules. The bulk purity of **1** was also confirmed by the PXRD study, which was well matched with the simulated pattern of the single-crystal X-ray diffraction data (Figure S2). The X-ray fluorescence spectrum of **1** showed the signals due to Au, S, and P, while no signal due to Cl was detected (Figure S3). The IR spectrum of **1** showed the ν_{P-C} bands due to dppe and the ν_{O-H}, and ν_{C-O} bands due to H_2tg^- (Figure S4) [29]. The ^{1}H NMR spectrum of **1** in $CDCl_3$ showed a multiplet signal at δ 7.66–7.46 ppm and a doublet signal at δ 2.69 ppm due to phenyl and methylene groups of dppe, respectively (Figure S5). Moreover, the ^{1}H NMR spectrum showed a multiplet signal at δ 3.80–3.64 ppm, three double-doublet signals at δ 3.66, 3.21, and 3.12 ppm, and two broad singlet signals at δ 3.50 and 2.35 ppm. The multiplet and double-doublet signals were due to the methylene and methine proton signals of H_2tg, and the broad singlet signals are assignable to the two hydroxy groups of H_2tg. The OH proton signals were slightly weak (1.6 or 1.5 H) compared to the expected value (2.0 H), which is probably because of the partial H/D exchange with $CDCl_3$ [30]. The integral intensity ratio of all signals implies the presence of dppe and H_2tg^- in a 1:2 ratio in **1**. The $^{31}P\{^1H\}$ NMR spectrum of **1** in $CDCl_3$ showed a singlet signal at δ 36.5 (Figure S6). Thus, **1** is characterized as a C_2 or C_s symmetrical linear digold(I) structure, as illustrated in Figure 1. Considering the chirality of two terminal H_2tg^- ligands (*R* or *S*), two diastereomers, the racemic (*RR*/*SS*) and the meso (*RS*) forms, are possible for **1**. However, the ^{1}H and ^{31}P NMR spectroscopy showed only a single set of signals for **1**, which implies that the selective formation of one of the two isomers or the rapid structural conversion between the two isomers occurs in solution.

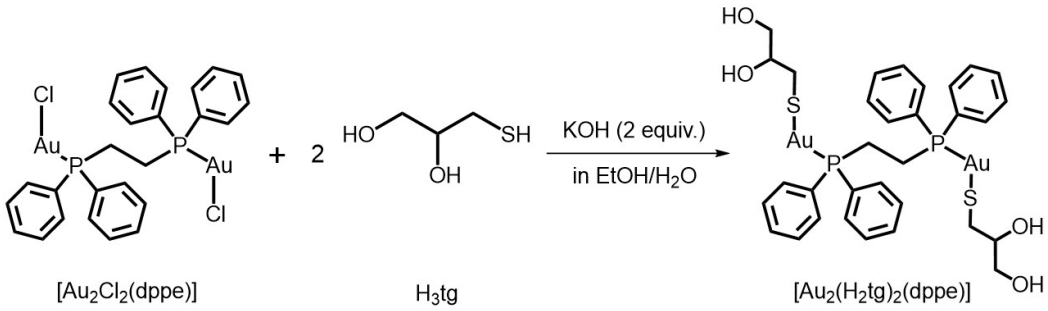


Figure 1. Synthetic route of **1**.

The diffuse reflectance spectrum of **1** showed a broad band at 330 nm in the solid state (Figure S7). While **1** was non-emissive at room temperature, **1** showed a photoluminescence centered at 496 nm at 77 K in the solid state (Figure S8). The emission quantum yield at 77 K was evaluated to be 8.3% using an integration sphere. The origin of the emission band was tentatively assigned to phosphorescence arising from a charge transfer transition from S to Au perturbed by aurophilic interaction (^{3}LMMCT), considering the assignment for related luminescent gold(I) complex with phosphine and thiolate ligands [31–38].

2.2. Crystal Structure of **1**

X-ray-quality single crystals of **1** were obtained from the filtrate after standing at room temperature for 1 day. Single-crystal X-ray analysis of **1** revealed that the asymmetric unit contains two Au^I, two halves of dppe, and two H_2tg^-. The symmetry expansion operation generated two crystallographically independent, but essentially the same, digold(I) complexes (molecules A and B) (Figure 2). Two gold(I) ions adopt an almost linear geometry by coordinating one S atom from H_2tg^- and one P atom from dppe. The dppe ligand bridges two Au^I ions in a μ_2-κ^2P,P' mode, while the H_2tg^- ligand binds to one Au^I center in a monodentate-κ*S* mode. The Au-S (2.3104(12), 2.304(10), and 2.293(15) Å) and Au-P (2.2652(9), 2.298(2), and 2.219(4) Å) bond distances and S-Au-P angles (175.81(4), 178.3(2), and 173.6(4) °) were within the range of related [Au_2(dppe)(thiolate-*S*)$_2$]-type dinuclear complexes [39–43]. The *R* and *S* isomers of H_2tg were disordered in a 0.65:0.35 ratio in both molecules A and B (Figure S9). Thus, discriminating between the racemic or meso isomers of **1** was difficult. In the crystal packing, molecules A and B were connected by the short Au···Au contact of 3.1237(19) and 3.132(3) Å, which is shorter than the sum of the VdW radii (3.32 Å) and suggestive of the presence of aurophilic interaction [26,27] (Figure S10). The ESI-mass spectrum of **1** in CH_2Cl_2/MeOH (v/v = 1/1) showed a dominant monovalent signal corresponding to the digold(I) complex molecule {[Au_2(dppe)(H_2tg)$_2$] + CH_2Cl_2 + Na}$^+$ at m/z = 1115, while no signal due to the polymeric species was detected (Figure S11). This observation means that the 1D polymer structure in **1** was dissociated in the solution.

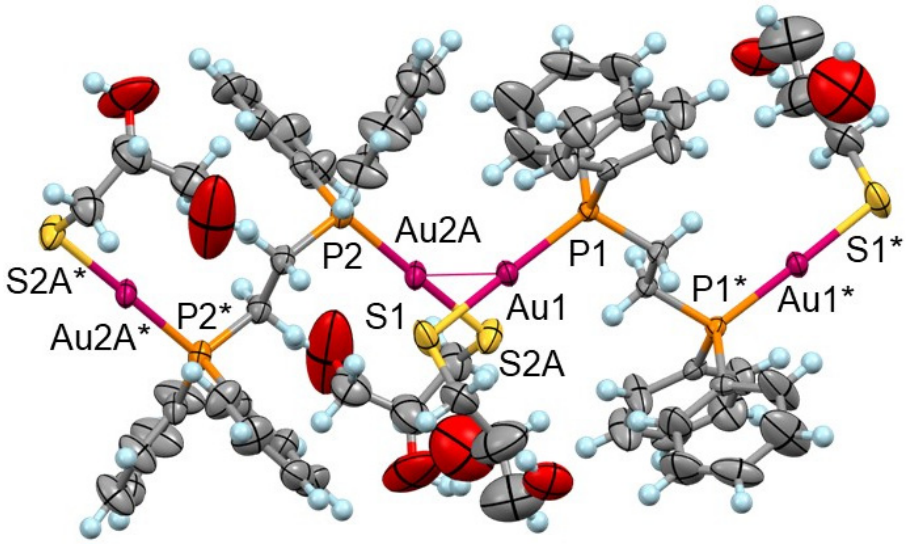


Figure 2. The extended structure of complex **1**. Molecules A and B contain Au1 and Au2, respectively. Disordered parts were omitted for clarity. The symbol (*) denotes the symmetry expanded atoms.

3. Materials and Methods

3.1. Materials

1-thioglycerol was kindly donated by Asahi Chemical Co., Ltd. (Osaka, Japan). [Au_2(dppe)Cl_2] was synthesized based on a literature method [28].

3.2. Physical Measurements

The IR spectrum was recorded with a JASCO FT/IR-4100 infrared spectrophotometer using the ATR method at room temperature. Elemental analyses (C, H, N) were performed at Osaka University using a Yanaco CHN Corder MT-5. High-quality powder X-ray diffraction (PXRD) was performed at 100 K in transmission mode (synchrotron radiation, λ = 0.8 Å; 2θ range = 2–78°; step width = 0.006°; data collection time 1 min) on a diffractometer equipped with an MYTHEN microstrip X-ray detector (Dectris Ltd., Baden, Switzerland) at the SPring-8 BL02B2 beamline [44]. The ground sample was placed in 0.3 mm glass capillary tubes. The samples were rotated during the measurements. ^{1}H

NMR spectra were recorded with a JEOL ECA500 (500 MHz) spectrometer in $CDCl_3$ with tetramethylsilane (TMS) as an internal standard. $^{31}P\{^1H\}$ NMR spectra were recorded with a JEOL ECA500 (500 MHz) spectrometer in $CDCl_3$, and chemical shifts (δ in ppm) were reported with reference to H_3PO_4. X-ray fluorescence spectrometry was performed on a SHIMADZU EDX-7000 spectrometer. The diffuse reflection spectrum was measured with a JASCO V-670 UV/Vis/NIR spectrometer. The photoluminescence spectra were recorded with a JASCO FP-8500 spectrometer at room temperature and 77 K. The internal emission quantum yield (Φ) was obtained via the absolute measuring method using an integrating sphere unit (JASCO ILFC-847), the internal surface of which was coated with highly reflective Spectralon. The ESC-842 calibrated light source (WI) and the ESC-843 calibrated light source (D2) were used to calibrate the emission intensities to measure the absolute quantum yields. The ESI-mass spectrum was measured in a positive mode using a Bruker micrOTOF II instrument.

3.3. X-ray Crystal Structure Determination

Diffraction data for the title compound **1** were recorded on a Rigaku XtaLAB Synergy Custom X-ray diffractometer equipped with a Hypix-6000HE hybrid photon-counting detector and a Rigaku VariMax rotating-anode X-ray source with a Mo target. The intensity data were processed using the CrysAlisPro program (version 1.171.41.122a) and collected using the ω-scan technique. The structures were solved by direct methods using SHELXS [45], and refined by SHELXL [45] using the Olex2 program [46]. H atoms were placed at the calculated positions and refined isotropically, while non-hydrogen atoms were refined anisotropically. The H_2tg ligands, dppe ligands, and gold atoms were positionally disordered over two positions, whose occupancy factors were refined to 0.648 and 0.352. Several DFIX, ISOR, DANG, and RIGU instructions were used to model the disordered parts. The crystallographic data and geometrical parameters of **1** were summarized in Figures S1 and S2.

*3.4. Synthesis of [$Au_2(H_2tg)_2$(dppe)] (**1**)*

[Au_2Cl_2(dppe)] was prepared by the reported method [28]. To a white suspension containing 500 mg of [Au_2Cl_2(dppe)] (0.577 mmol) in EtOH (75 mL), 125 mg of 1-thioglycerol (1.16 mmol) in 11.3 mL of 0.2 M aqueous KOH solution was added. The smoky white mixture was stirred at room temperature in the dark for 3 h, and the resulting pale-yellow precipitate of **1** was collected by filtration. Yield: 277 mg (47%). IR spectrum, ν, cm^{-1}: 3376 (ν_{O-H}), 1482, 1435 (ν_{P-CH2-}), 1409, 1103 (ν_{P-Ph}), 1067 (ν_{C-O}), 1027 (ν_{C-O}), 731 (ν_{P-CH2-}), and 691 (ν_{P-Ph}). ^1H NMR spectrum ($CDCl_3$, 500 MHz), δ: 7.66–7.46 (20H, m), 3.80–3.64 (4H, m), 3.66 (2H, dd, *J* = 11.2, 5.9 Hz), 3.50 (1.6H, s), 3.21 (2H, dd, *J* = 13.0, 4.2 Hz), 3.12 (2H, dd, *J* = 13.0, 7.9 Hz), 2.69 (4H, d, *J* = 1.7 Hz), and 2.35 (1.5H, s). $^{31}P\{^1H\}$ NMR spectrum ($CDCl_3$, 202 MHz), δ: 36.5 (s). Anal. Calcd. for [$Au_2(H_2tg)_2$(dppe)] = $C_{32}H_{38}Au_2O_4P_2S_2$ (Mw = 1006.66): C, 38.18%; H, 3.80%. Found: C, 38.14%; H, 3.86%.

4. Conclusions

In conclusion, we synthesized a new dinuclear Au^I complex **1** from the reaction of [Au_2Cl_2(dppe)] with H_3tg/KOH in a 1:2 ratio. Single-crystal X-ray analysis revealed that two H_2tg^- ligands bind to the linear $[Au^I_2(dppe)]^{2+}$ unit through the Au-S coordination bonds in **1**. In the crystal packing, the digold(I) complex **1** is infinitely connected through the intermolecular aurophilic interactions to form a 1D polymeric supramolecular structure. Due to the presence of aurophilic interactions, the solid sample of **1** showed a photoluminescence at 77 K. It should be noted that **1** is the first example of the metal complex having H_2tg^- ligands in a non-bridging κ*S* coordination mode. It has been known that the non-bridging thiolato groups can bind to secondary metal ions to form S-bridged multinuclear complexes [25,47,48]. Thus, the reactivity of complex **1** with transition metal ions is undergoing in our group.

Supplementary Materials: The following supporting information is available: Figure S1: Structurally characterized metal complexes with H_3tg. (a) $[Cd(\mu\text{-}H_2tg\text{-}S)_2]_\infty$ [19]. (b) $[Au_2(PPh_3)_3(\mu\text{-}H_2tg\text{-}S)]$ [20]. (c) $[Zn(H_2tg\text{-}S,O)(Tp^{PhMe})]$ [21]. (d) $[Ln_2(ClP)_2(H_3tg\text{-}O)_2(H_2O)_2]$ (Ln = Nd, Eu) [22,23]; Figure S2: (a) Observed and (b) simulated powder X-ray diffraction patterns of **1**; Figure S3: X-ray fluorescence spectrum of **1**; Figure S4: IR spectrum of **1**; Figure S5: ^{1}H NMR spectrum of **1** in $CDCl_3$. The symbol (*) denotes signals from ethanol, $CHCl_3$, and H_2O; Figure S6: $^{31}P\{^1H\}$ NMR spectrum of **1** in $CDCl_3$; Figure S7: Diffuse reflection spectrum of **1**; Figure S8: Emission (solid line) and excitation (dashed line) spectra of **1** at room temperature (black) and at 77 K (red) in the solid state; Figure S9: A perspective view of (top) molecules A and (bottom) B in **1**; Figure S10: Packing structure of **1**; Figure S11: ESI-mass spectrum of **1** in CH_2Cl_2/MeOH. Inset: Simulated and observed pattern for the signal at m/z = 1115.06; Table S1: Crystallographic data for **1**; Table S2: Selected bond distances and angles for **1**. CCDC 2276216 contains the supplementary crystallographic data for this paper.

Author Contributions: Methodology, T.B.; validation, N.Y.; formal analysis, T.B.; data curation, T.B.; writing—original draft preparation, T.B. and N.Y.; writing—review and editing, N.Y.; visualization, T.B.; supervision, N.Y. All authors have read and agreed to the published version of the manuscript.

Funding: This work was supported in part by JSPS KAKENHI (Grant No. 19K05496) and by Asahi Chemical Co., Ltd. (Osaka, Japan).

Data Availability Statement: The spectroscopic data presented in this study are available as supplementary materials.

Acknowledgments: We sincerely thank Asahi Chemical Co., Ltd. (Osaka, Japan) for the gift of 1-thioglycerol. This work was the result of using research equipment shared in the MEXT Project for promoting the public utilization of advanced research infrastructure (a program for supporting the construction of core facilities) (Grant Number JPMXS0441200023).

Conflicts of Interest: The authors declare no conflict of interest. The funders had no role in the design of the study; in the collection, analyses, or interpretation of data; in the writing of the manuscript; or in the decision to publish the results.

References

1. Kazuhara, A. A Raman spectroscopic investigation of the mechanism of the reduction in hair with thioglycerol and the accompanying disulphide conformational changes. *Int. J. Cosmet. Sci.* **2018**, *40*, 34–43. [CrossRef] [PubMed]
2. Seltzer, W.K.; Dhariwal, G.; McKelvey, H.A.; McCabe, E.R.B. 1-thioglycerol: Inhibitor of glycerol kinase activity in vitro and in situ. *Life Sci.* **1986**, *39*, 1417–1424. [CrossRef]
3. Vossmeyer, T.; Katsikas, L.; Giersig, M.; Popovic, I.G.; Chemseddine, A.; Eychmüller, A.; Weller, H. CdS Nanoclusters: Synthesis, Characterization, Size Dependent Oscillator Strength, Temperature Shift of the Excitonic Transition Energy, and Reversible Absorbance Shift. *J. Phys. Chem.* **1994**, *98*, 7665–7673. [CrossRef]
4. Rogach, A.L.; Kornowski, A.; Gao, M.; Eychmüller, A. Horst Weller Synthesis and Characterization of a Size Series of Extremely Small Thiol-Stabilized CdSe Nanocrystals. *J. Phys. Chem. B* **1999**, *103*, 3065–3069. [CrossRef]
5. Silva, A.C.A.; da Silva, S.W.; Morais, P.C.; Dantas, N.O. Shell Thickness Modulation in Ultrasmall $CdSe/CdS_xSe_{1-x}/CdS$ Core/Shell Quantum Dots via 1-Thioglycerol. *ACS Nano* **2014**, *8*, 1913–1922. [CrossRef] [PubMed]
6. Rogach, A.L.; Katsikas, L.; Kornowski, A.; Su, D.; Eychmüller, H.A. Eychmüller; H. Weller Synthesis and characterization of thiol-stabilized CdTe nanocrystals. *Berich. Bunsen. Gesell.* **1996**, *100*, 1772–1778. [CrossRef]
7. Dhobale, S.; Thite, T.; Laware, S.L.; Rode, C.V.; Koppikar, S.J.; Ghanekar, R.-K.; Kale, S.N. Zinc oxide nanoparticles as novel alpha-amylase inhibitors. *J. Appl. Phys.* **2008**, *104*, 094907. [CrossRef]
8. Kumbhojkar, N.; Nikesh, V.V.; Kshirsagar, A.; Mahamuni, S. Photophysical properties of ZnS nanoclusters. *J. Appl. Phys.* **2000**, *88*, 6260–6264. [CrossRef]
9. Kim, H.; Cho, K.; Song, H.; Min, B.; Lee, J.-S.; Kim, G.-T.; Kim, S.; Kim, S.H.; Noh, T. Photocurrent mechanism in a hybrid system of 1-thioglycerol-capped HgTe nanoparticles. *J. Appl. Phys.* **2003**, *83*, 4619–4621. [CrossRef]
10. Kumaria, Y.; Jangir, L.K.; Kumar, A.; Kumara, M.; Awasthi, K. Investigation of thermal stability of TiO_2 nanoparticles using 1-thioglycerol as capping agent. *Solid State Commun.* **2017**, *263*, 1–5. [CrossRef]
11. Gaia, I.A.T.; Guimarães, E.V.; Maia, P.I.S.; Mikhail, H.D.; da Luz, M.S.; S, A.C.A.; Silva, R.S. Synthesis and investigation of optical and structural properties of Bi_2O_3/Bi_2S_3 nanoparticles in an aqueous solution. *Physica B* **2023**, *662*, 414947. [CrossRef]
12. Chai, O.J.H.; Wu, Z.; Xie, J. All Hydroxyl-Thiol-Protected Gold Nanoclusters with Near-Neutral Surface Charge. *J. Phys. Chem. Lett.* **2021**, *12*, 9882–9887. [CrossRef] [PubMed]
13. Schneider, C.M.; Cölfen, H. Formation of Nanoclusters in Gold Nucleation. *Crystals* **2020**, *10*, 382. [CrossRef]
14. Yao, H.; Yaomura, S. Emergence of Large Chiroptical Responses by Ligand Exchange Cross-Linking of Monolayer-Protected Gold Clusters with Chiral Dithiol. *Langmuir* **2013**, *29*, 6444–6451. [CrossRef] [PubMed]

15. Sumi, T.; Motono, S.; Ishida, Y.; Shirahata, N.; Yonezawa, T. Formation and Optical Properties of Fluorescent Gold Nanoparticles Obtained by Matrix Sputtering Method with Volatile Mercaptan Molecules in the Vacuum Chamber and Consideration of Their Structures. *Langmuir* **2015**, *31*, 4323–4329. [CrossRef] [PubMed]
16. Komarov, V.P.; Lazarev, V.B.; Shaplygin, I.S. Preparation and thermal decomposition of complexes of silver(I) and gold(I) with thiovanol. *Zhurnal Neorg. Khimii* **1980**, *25*, 746–751.
17. Nigam, H.L.; Kumar, A.N.; Pandeya, K.B. Infrared absorption spectra of metal complexes of some sulfur containing ligands. *Proc. Chem. Symp.* **1970**, *2*, 53–57.
18. Hager, C.-D.; Huber, F. (Hydroxyalkyl)- und (4-Hydroxyphenyl)organoplumbylsulfide. *Z. Naturforsch.* **1980**, *35*, 931–933. [CrossRef]
19. Vossmeyer, T.; Reck, G.; Katsikas, L.; Haupt, E.T.K.; Schulz, B.; Weller, H. A New Three Dimensional Crystal Structure of a Cadmium Thiolate. *Inorg. Chem.* **1995**, *34*, 4926–4929. [CrossRef]
20. López-de-Luzuriaga, J.M.; Sladek, A.; Schmidbaur, H. Mixed coordination numbers and geometries of gold(I) in a dinuclear complex of thioglycerol. *J. Chem. Soc. Dalton Trans.* **1996**, 4511–4512. [CrossRef]
21. Tekeste, T.; Vahrenkamp, H. Modeling zinc enzyme inhibition with functional thiolate ligands. *Inorg. Chem.* **2006**, *45*, 10799–10806. [CrossRef] [PubMed]
22. Kyprianidou, E.J.; Lazarides, T.; Kaziannis, S.; Kosmidis, C.; Itskos, G.; Manos, M.J.; Tasiopoulos, A.J. Single crystal coordinating solvent exchange as a general method for the enhancement of the photoluminescence properties of lanthanide MOFs. *J. Mater. Chem. A* **2014**, *2*, 5258–5266. [CrossRef]
23. Manos, M.J.; Kyprianidou, E.J.; Papaefstathiou, G.S.; Tasiopoulos, A.J. Insertion of Functional Groups into a Nd^{3+} Metal–Organic Framework via Single-Crystal-to-Single-Crystal Coordinating Solvent Exchange. *Inorg. Chem.* **2012**, *51*, 6308–6314. [CrossRef] [PubMed]
24. Dance, I.G. The structural chemistry of metal thiolate complexes. *Polyhedron* **1986**, *5*, 1037–1104. [CrossRef]
25. Yoshinari, N.; Konno, T. Metallosupramolecular Structures Derived from a Series of Diphosphine-bridged Digold(I) Metalloligands with Terminal D-Penicillamine. *Chem. Rec.* **2016**, *16*, 1647–1663. [CrossRef]
26. Pyykkö, P. Strong Closed-Shell Interactions in Inorganic Chemistry. *Chem. Rev.* **1997**, *97*, 597–636. [CrossRef]
27. Schmidbaur, H.; Schier, A. A briefing on aurophilicity. *Chem. Soc. Rev.* **2008**, *37*, 1931–1951. [CrossRef]
28. Mirabelli, C.K.; Hill, D.T.; Faucette, L.F.; McCabe, F.L.; Girard, G.R.; Bryan, D.B.; Sutton, B.M.; Bartus, J.O.; Crooke, S.T.; Johnson, R.K. Antitumor Activity of Bis(diphenylphosphino)alkanes, Their Gold(I) Coordination Complexes, and Related Compounds. *J. Med. Chem.* **1987**, *30*, 2181–2190. [CrossRef]
29. Socrates, G. *Infrared Characteristic Group Frequencies*, 3rd ed.; Wiley: Chichester, UK, 2001.
30. Sabot, C.; Kumar, K.A.; Antheaume, C.; Mioskowski, C. Triazabicyclodecene: An Effective Isotope Exchange Catalyst in $CDCl_3$. *J. Org. Chem.* **2007**, *72*, 5001–5004. [CrossRef]
31. Tzeng, B.-C.; Liao, J.-H.; Lee, G.-H.; Peng, S.-M. Photophysical properties, electronic and crystal structures of luminescent diphosphine digold(I)-pyridine-2-thiolate complexes. *Inorg. Chim. Acta* **2004**, *357*, 1405–1410. [CrossRef]
32. Li, C.-K.; Lu, X.-X.; Wong, K.M.-C.; Chan, C.-L.; Zhu, N.; Yam, V.W.-W. Molecular Design of Luminescence Ion Probes for Various Cations Based on Weak Gold(I)···Gold(I) Interactions in Dinuclear Gold(I) Complexes. *Inorg. Chem.* **2004**, *43*, 7421–7430. [CrossRef] [PubMed]
33. Bardají, M.; Calhorda, M.J.; Costa, P.J.; Jones, P.G.; Laguna, A.; Pérez, M.R.; Villacampa, M.D. Synthesis, Structural Characterization, and Theoretical Studies of Gold(I) and Gold(I)−Gold(III) Thiolate Complexes: Quenching of Gold(I) Thiolate Luminescence. *Inorg. Chem.* **2006**, *45*, 1059–1068. [CrossRef] [PubMed]
34. Costa, P.J.; Calhorda, M.J. A DFT and MP2 study of luminescence of gold(I) complexes. *Inorg. Chim. Acta* **2006**, *359*, 3617–3624. [CrossRef]
35. Schneider, J.; Lee, Y.-A.; Pérez, J.; Brennessel, W.W.; Flaschenriem, C.; Eisenberg, R. Strong Intra- and Intermolecular Aurophilic Interactions in a New Series of Brilliantly Luminescent Dinuclear Cationic and Neutral Au(I) Benzimidazolethiolate Complexes. *Inorg. Chem.* **2008**, *47*, 957–968. [CrossRef] [PubMed]
36. Tiekink, E.R.T.; Kang, J.-G. Luminescence properties of phosphinegold(I) halides and thiolates. *Coord. Chem. Rev.* **2009**, *253*, 1627–1648. [CrossRef]
37. Koshevoy, I.O.; Smirnova, E.S.; Haukka, M.; Laguna, A.; Chueca, J.C.; Pakkanen, T.A.; Tunik, S.P.; Ospino, I.; Crespo, O. Synthesis, structural characterization, photophysical properties and theoretical analysis of gold(I) thiolate-phosphine complexes. *Dalton Trans.* **2011**, *40*, 7412–7422. [CrossRef]
38. Crespo, O.; Gimeno, M.C.; Laguna, A.; Lahoz, F.J.; Larraz, C. Unprecedented Luminescent Heteropolynuclear Aggregates with Gold Thiolates as Building Blocks. *Inorg. Chem.* **2011**, *50*, 9533–9544. [CrossRef]
39. Moreno-Alcántar, G.; Romo-Islas, G.; Flores-Álamo, M.; Torrens, H. Aurophilicity vs. thiophilicity: Directing the crystalline supramolecular arrangement in luminescent gold compounds. *New J. Chem.* **2018**, *42*, 7845–7852. [CrossRef]
40. Onaka, S.; Yaguchi, M.; Yamauchi, R.; Ozeki, T.; Ito, M.; Sunahara, T.; Sugiura, Y.; Shiotsuka, M.; Nunokawa, K.; Horibe, M.; et al. The effect of carbon chain length of the diphosphine ligand on the aurophilic interaction. Synthesis and X-ray structural study for a series of Au(I) compounds with Ph_2P–R–PPh_2 and *S*-$(CH_2)_n$-py ligands. *J. Organomet. Chem.* **2005**, *690*, 57–68. [CrossRef]

41. Artigas, M.M.; Crespo, O.; Gimeno, M.C.; Jones, P.G.; Laguna, A.; Villacampa, M.D. Gold(I) complexes with the ligand 1-thiolate-1,2-dicarba-*closo*-dodecaborate. Crystal structure of $[Au_2(1\text{-}S\text{-}1,2\text{-}C_2B_{10}H_{11})_2(\mu\text{-dppe})]$. *J. Organomet. Chem.* **1998**, *561*, 1–6. [CrossRef]
42. Ho, S.Y.; Cheng, E.C.-C.; Tiekink, E.R.T.; Yam, V.W.-W. Luminescent Phosphine Gold(I) Thiolates: Correlation between Crystal Structure and Photoluminescent Properties in $[R_3PAu\{SC(OMe)=NC_6H_4NO_2\text{-}4\}]$ (R = Et, Cy, Ph) and $[(Ph_2P\text{-}R\text{-}PPh_2)\{AuSC(OMe)=NC_6H_4NO_2\text{-}4\}_2]$ (R = CH_2, $(CH_2)_2$, $(CH_2)_3$, $(CH_2)_4$, Fc). *Inorg. Chem.* **2006**, *45*, 8165–8174. [CrossRef] [PubMed]
43. Ilie, A.; Raţ, C.I.; Scheutzow, S.; Kiske, C.; Lux, K.; Klapötke, T.M.; Silvestru, C.; Karaghiosoff, K. Metallophilic Bonding and Agostic Interactions in Gold(I) and Silver(I) Complexes Bearing a Thiotetrazole Unit. *Inorg. Chem.* **2011**, *50*, 2675–2684. [CrossRef] [PubMed]
44. Kawaguchi, S.; Takemoto, M.; Osaka, K.; Nishibori, E.; Moriyoshi, C.; Kubota, Y.; Kuroiwa, Y.; Sugimoto, K. High-throughput powder diffraction measurement system consisting of multiple MYTHEN detectors at beamline BL02B2 of SPring-8. *Rev. Sci. Instrum.* **2017**, *88*, 085111. [CrossRef] [PubMed]
45. Sheldrick, G.N. Crystal Structure Refinement with SHELXL. *Acta Cryst.* **2015**, *C71*, 3–8.
46. Dolomanov, O.V.; Bourhis, L.J.; Gildea, R.J.; Howard, J.A.K.; Puschmann, H. OLEX2: A complete structure solution, refinement and analysis program. *J. Appl. Cryst.* **2009**, *42*, 339–341. [CrossRef]
47. Yoshinari, N.; Konno, T. Chiral Phenomena in Multinuclear and Metallosupramolecular Coordination Systems Derived from Metalloligands with Thiol-containing Amino Acids. *Bull. Chem. Soc. Jpn.* **2018**, *91*, 790–812. [CrossRef]
48. Yoshinari, N.; Kuwamura, N.; Kojima, T.; Konno, T. Development of Coordination Chemistry with Thiol-containing Amino Acids. *Coord. Chem. Rev.* **2023**, *474*, 214857. [CrossRef]

Disclaimer/Publisher's Note: The statements, opinions and data contained in all publications are solely those of the individual author(s) and contributor(s) and not of MDPI and/or the editor(s). MDPI and/or the editor(s) disclaim responsibility for any injury to people or property resulting from any ideas, methods, instructions or products referred to in the content.